The Astronomical Journal, 149:109 (6pp), 2015 March
doi:10.1088/0004-6256/149/3/109

TRANSIENT CARBON MONOXIDE (CO) ABSORPTION AND PERSISTENT BRACKETT ALPHA (Brα) EMISSION IN THE SPECTRUM OF ϵ AURIGAE

R. E. Stencel[1], R. D. Blatherwick[1], and T. R. Geballe[2]
[1] Department of Physics and Astronomy, University of Denver, Denver, CO 80208, USA
[2] Gemini Observatory, 670 N. A'ohoku Place, Hilo, HI 96720, USA
Received 2014 February 9; accepted 2015 January 12; published 2015 February 26

ABSTRACT

We obtained high-resolution infrared spectroscopy of the long period binary, ϵ Aurigae, in the vicinity of the near-infrared overtone band of CO, at four epochs during 2011–2012. These observations span the period from late phase of the recent eclipse, to after the eclipse. Lines of both ^{12}CO and ^{13}CO were observed, confirming the report from the 1983 eclipse that these features were present during the second half of the eclipse. The bands were absent post-eclipse, consistent with their formation only in the several AU diameter disk that has been shown to cause the eclipse. We fitted the eclipse spectra with CO column densities 8×10^{19} cm^{-2} at 1275 K when nearer to mid-eclipse, and 1.5×10^{20} cm^{-2} at 1050 K during third contact. We also found that $^{12}C/^{13}C = 5 \pm 1$ in the disk. Assuming that mass transfer from the primary star formed the disk, this implies a helium core burning evolutionary state for the primary star. We also obtained a high-resolution post-eclipse spectrum of the 4.05 μm Brackett α emission line. The small radial velocity difference of the emission, relative to a nearby photospheric line of primary star origin, indicates that the emission may arise from nearer the system center of mass, such as a recombination region larger than the immediate vicinity of the unseen companion star surrounded by the disk. The combination of CO and Brα lines provides important diagnostics for resolving ongoing questions about the evolutionary state of this system.

Key words: accretion, accretion disks – binaries: eclipsing – binaries: general – infrared: general – stars: individual (epsilon Aurigae)

Supporting material: data behind figures

1. INTRODUCTION

The bright star, ϵ Aurigae, is an SB1 eclipsing binary system with a 27.1 yr period. The primary star appears to be an F supergiant, which shows ~0.1 mag light variations with a quasi-period of 67 days. This system is the brightest member of a recently defined class of binary stars with disk-eclipse phenomena (Hajduk et al. 2008; Herbst et al. 2008). The long unseen companion has been detected using near-infrared interferometric imaging and exhibits a disk-like shape with a dimension of several AU (Kloppenborg et al. 2010). This disk probably surrounds an upper main sequence star, based on likely binary star mass ratios, transient He 10830 Å absorption, and a far-UV excess. Based on a suite of measurements made during the 2010–11 eclipse (cf. Stencel 2012), the disk itself resembles a photo-evaporating or transitional disk in the classification of disks outlined by Williams & Cieza (2011). The observations have also confirmed the suggestion by Takeuchi (2011) that the temperature of the side of the disk facing away from the primary star, as seen during the eclipse, is 550 K, whereas the temperature of that portion of the disk facing the primary star, visible during secondary minimum as seen from Earth, is 1100 K—see Stencel et al. (2011) and Hoard et al. (2012) for details. This range of conditions suggests that thermally driven phase changes could occur in any solid state material within the disk. The strength and variations of strong spectral features of sodium and potassium seen during eclipse suggests thermal effects extend to these 1000 K volatile alkali elements as well (Leadbeater et al. 2012).

Observations obtained during the prior eclipse, in 1984, by Hinkle & Simon (1987; hereafter HS87) revealed transient carbon monoxide (CO) absorption lines from its first overtone band near 2.3 μm. Those authors interpreted the CO as arising in the disk associated with the unseen companion. They derived an isotopic ratio, $^{12}C/^{13}C = 10 \pm 3$, indicating that the disk may contain material recently accreted from the post-main sequence primary star. This, along with the lack of extended infrared shells (Hoard et al. 2012), indicates the primary star may have only recently evolved away from the upper main sequence, and is partway through its first-crossing of the HR diagram.

We have obtained high resolution spectra of ϵ Aur in the long wavelength portion of the K band (2.3–2.4 μm) during and after the 2010 eclipse. The principal goal was to explore details of the CO band re-appearance, and in particular to evaluate the prior report that ^{13}C was present at a level suggestive of an evolutionary status of core helium burning and dredge-up.

We also have obtained a post-eclipse spectrum including the H I Brackett α (Br α, 5–4) and Humphreys θ (Hu θ, 14–6) lines at 4.05 and 4.02 μm, respectively. The original goal was to use the observed velocity difference in these lines to constrain the mass of the unseen companion.

The Br α line has been seen consistently in emission in a series of low resolution IRTF/SpeX observations outside and during eclipse during 2008–2011—see Figure 1 in Stencel et al. (2011). This emission line is also present in older narrow-band FTS data; e.g., see Figure 4 in Backman et al. (1985). Similarly, *Spitzer* IRS data obtained in 2005–2006 showed the α transition of the Humphreys series (H I 7–6) at 12.37 μm to also be in emission (Stencel 2007). These two terminal recombination lines appear to be optically thin and symmetric when viewed at medium resolution, and thus ideally might be

Table 1
ϵ Aurigae Observing Log

UT Date, RJD	Days After Mid-eclipse	Phase	λ (μm)	Exp Time (s)	Tell. Std.	Program	Comment
20110104, 55565	165	totality	2.26–2.37	400	HD 34759	GN-2010B-SV-46	CO + Pfund series
20110330, 55650	250	3rd contact	2.29–2.35	360	HD 32630	GN-2010B-SV-46	CO + Pfund series
20110412, 55663	263	3rd contact	2.29–2.35	360	HD 32630	GN-2010B-SV-46	CO + Pfund series
20120418, 56035	269	post-eclipse	2.28–2.38	1024	HIP 25413	GN-2012A-DD-3	Pfund series only
20121221, 56283	882	post-eclipse	3.985–4.075	128	HD 34759	GN-2012B-DD-4	Br α and Hu θ

RJD = JD-2,400,000

usable as velocity tracers of the companion, assuming the emission arises from the vicinity of the hot companion, e.g., from disk accretion energy. Other higher lying hydrogen recombination lines (e.g., the rest of the Balmer, Paschen, Brackett, and Pfund series) are seen mainly in absorption, apparently dominated by formation in the F star photosphere. Balmer α at 0.6563 μm exhibits strongly variable emission wings around a wide and shallow absorption core, complicating velocity analysis. Paschen α (1.8756 μm) and Pfund α (7.4599 μm) are difficult to measure due to strong telluric absorption. Thus, Br α and nearby Hu θ appear to offer the best possibility for measuring differences in radial velocity between the binary components. We observed them post-eclipse, when the velocity separation of components was predicted to be approaching a maximum.

The scientific questions addressed by this paper include: (1) what is the nature of a disk's atmosphere (revealed by transient CO) and (2) what is the mass ratio of this binary star plus disk system (explored with Brackett alpha)? The respective importance of these questions, and this effort, include: (1) using CO parameters to elucidate transient atmospheric conditions, seen in this case and only in this molecule, as a tracer for the physical conditions in this disk, and (2) using radial velocity measurements to determine the masses involved, and hence the evolutionary state of this system. Implications of this work include: (1) whether this disk represents an early or late stage as a transitional disk, as well as (2) whether mass transfer in this binary could have caused a reversal of the mass ratio. This paper reports on one of the few binary star systems where disk atmospheric changes can be measured, which can be relevant to exoplanet atmospheric studies. Also, evidence about the mass ratio can resolve a long-standing problem in studies of this particular binary star. Section 2 summarizes the observations and data reduction. Section 3 provides a description of the observed CO and hydrogen recombination line spectra. Section 4 reports our analysis of these spectra. Conclusions are given in Section 5.

2. OBSERVATIONS AND DATA REDUCTION

All spectra were obtained at the Frederick C. Gillett Gemini North Telescope for programs GN-2010B-SV-146, GN-2012A-DD-3, and GN-2012B-DD-4, each of which used the facility near-infrared spectrograph GNIRS in its highest resolution configuration: 111 line/mm grating, long focal length camera, and 0.10 arcsec wide slit. Spectral resolving powers were 19,000 at 2.3 μm and 22,000 at 4.05 μm. An observing log is provide in Table 1. The spectra were obtained in the standard stare/nod manner. Early type telluric standards included η Aur and HD 34759, at nearly identical airmass to ϵ Aur, and observed either just prior to, or just after ϵ Aur.

Data reduction steps included flat-field division, spike removal, rectification, and extraction using standard IRAF and Figaro routines. Wavelength calibration was achieved using combinations of telluric absorption lines and arc lamp emission lines. The accuracy of the wavelength calibration is ~0.00002 μm at 2.3–2.4 μm and ~0.00003 μm at 4.05 μm, corresponding to a velocity uncertainty of $\pm 2\,\mathrm{km\,s^{-1}}$ for each line.

The intrinsic spectra of the telluric standards are essentially featureless in the 2.3–2.4 μm interval. In the wavelength interval near 4.05 μm, however, the spectrum of the telluric standard contains contains a strong Br α absorption line. The spectrum also has a large number of narrow telluric absorption lines, mostly of N_2O. To remove the Br α line from the spectrum of the telluric standard, an artificial spectrum linearly interpolated across each N_2O line in the vicinity of the Br α absorption profile was created and divided into the spectrum of the standard. The resulting spectrum, now devoid of the Br α line but retaining the telluric lines, was then used to ratio the spectrum of ϵ Aur and remove the telluric features. We see no residual systematic emission or absorption features in the ratio spectrum at the wavelengths of the N_2O lines. This technique allowed the recovery of the profile of the Br α line in ϵ Aur.

3. RESULTS

3.1. The 2.3–2.4 μm Spectra

Figure 1 shows the normalized reduced 2.3–2.4 μm spectra obtained in 2011 and 2012. The top three spectra were obtained during the eclipse, whereas the bottom spectrum was obtained post-eclipse. The spectra during eclipse are dominated by CO lines, but they also contain weak hydrogen Pfund series lines, presumed to be formed in the primary, which, as can be seen in the post-eclipse spectrum in Figure 1, are present above the noise level at wavelengths of 2.33 μm and longer. The CO absorption lines in the top spectrum of Figure 1, obtained in 2011 January, are only about two-thirds of the depths of the lines in the spectra from 2011 late March and mid-April, indicating that either a larger fraction of the later line of sight to the primary star was occulted by the disk or that the later line of sight passed through an optically thicker portion of the disk, in terms of the CO column density.

At all three epochs during the eclipse lines of ^{12}CO are present from both the 2–0 and 3–1 vibrational transitions. Lines from the 2–0 band of ^{13}CO are seen in the spectrum from 2011 January 4 and can readily be identified in the expanded portion of the spectrum shown in Figure 2. The spectral coverage in 2011 March and April only barely extended into the wavelength region where lines of ^{13}CO occur.

In late-type stellar atmospheres, the heads of the CO bands (e.g., at 2.294, 2.323, and 2.345 μm for ^{12}CO 2–0 and 3–1 and ^{13}CO 2–0, respectively), which occur at $J = 50$, produce

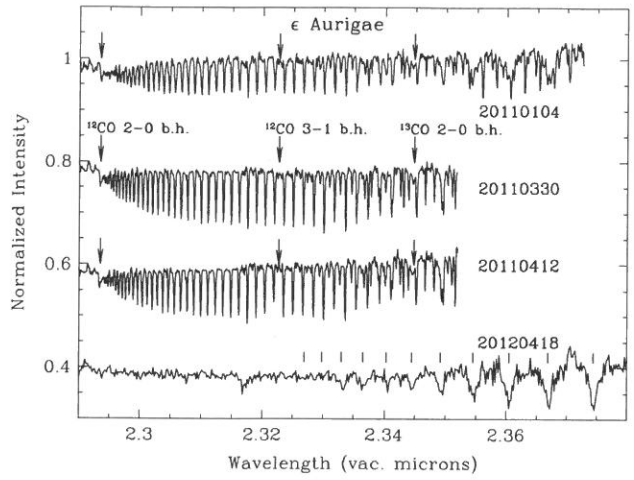

Figure 1. Spectra of ϵ Aur in the 2.3–2.4 μm interval at four epochs (intensity offset by 0.2 for clarity and dates given in UT). The wavelengths of the first two bandheads of ^{12}CO and the first bandhead of ^{13}CO are indicated by arrows. The spectrum obtained on 20120418 has been binned into intervals of 0.0002 μm; wavelengths of Pfund series lines are indicated by vertical lines. The spurious feature at 2.317 μm is due to incomplete correction of a strong telluric band. The data used to create this figure are available.

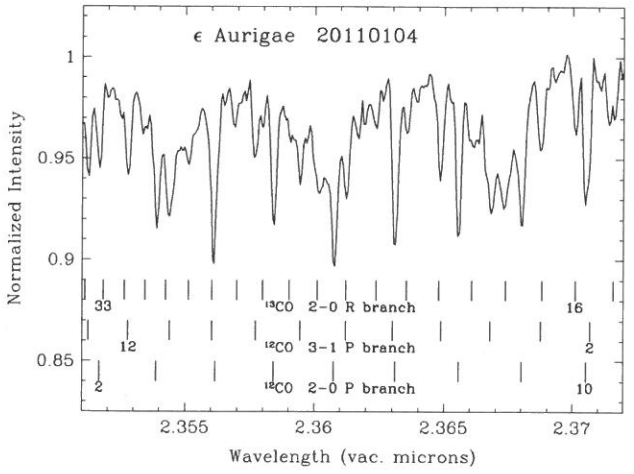

Figure 2. Details of spectrum of ϵ Aur at 2.35–2.37 μm on UT 2011 Jan 4. The laboratory wavelengths of overtone band lines of ^{12}CO and ^{13}CO are indicated; the numbers refer to R or P branch transitions. The spectrum has been shifted by +0.00017 μm into the laboratory frame of reference. The broad features are H Pfund lines.

considerably stronger absorptions than individual isolated lines. The opposite is the case for ϵ Aur. For example, the ^{12}CO 2–0 bandhead is only one-third the depth of the strongest individual lines. This indicates that the absorbing gas, although warm and dense, is at considerably lower temperature than a stellar photosphere, as is deduced below. The ^{13}CO 2–0 bandhead is not evident at all; the weak absorption feature at that wavelength is due to the H Pfund 30–5 transition, which can be clearly seen in the post-eclipse spectrum in Figure 1 and in Figure 2.

At each epoch where the CO lines were detected, the widths are slightly larger than the spectral resolution, and indicate that the intrinsic FWHMs of the lines are 10–15 km s^{-1}, consistent with the results of HS87. The heliocentric velocities of peak absorption in the ^{12}CO 2–0 band lines are constant with lower state energy to within the uncertainty ($\pm$2 km s^{-1}) for the

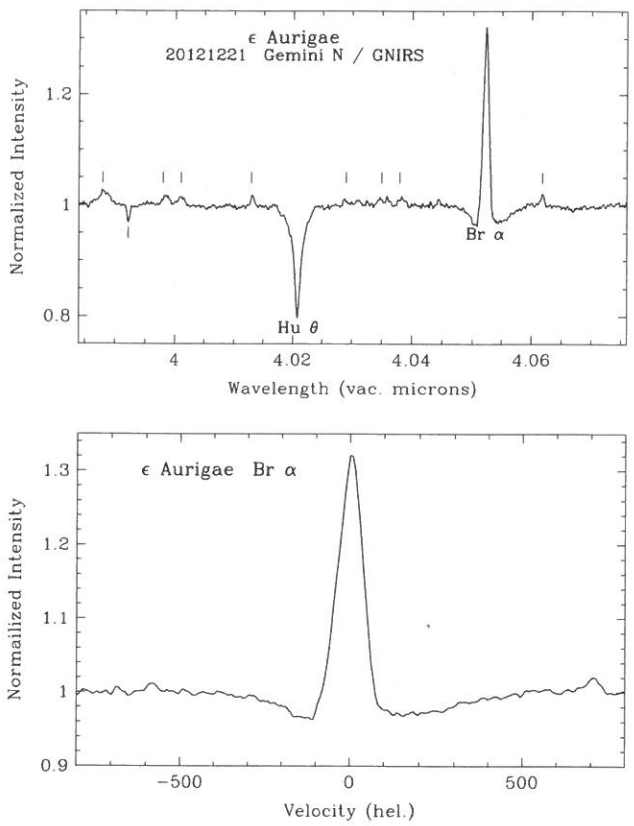

Figure 3. Top panel: post-eclipse spectrum of ϵ Aur at 3.98–4.08 μm obtained on UT 2012 December 21, showing the photospheric Hu θ absorption and emission/absorption from the Brackett α line, along with small emission lines marked with short vertical lines. Lower panel: the Brackett α line in velocity space. The data used to create this figure are available.

strong ^{12}CO 2–0 band lines. Based on the laboratory wavelengths of these lines, calculated using the constants from Mantz et al. (1975), the velocity of the CO absorption was –34 km s^{-1} on 2011 January 4, –43 km s^{-1} on March 30, and –45 km s^{-1} on April 12. These velocities are consistent with disk rotation profiles described by changes seen in the disk-tracer neutral potassium line at 7699 Å (Leadbeater et al. 2012).

3.2. The 4 μm Spectrum

Figure 3 shows the reduced and normalized spectrum of ϵ Aur near 4 μm. The most prominent features are the Br α emission and Hu θ absorption lines. The Br α emission sits on a broad absorption trough and rises 30% above the adjacent continuum. To determine the line centers, Gaussian functions were used to fit the line cores. As expected, Hu θ shows no indication of emission; its absorption core is sharp. Based on the vacuum rest wavelengths of 4.05227 μm for Br α and 4.02087 μm for Hu θ (from the NIST Atomic Spectra Database), the heliocentric peak emission (Br α) and absorption (Hu θ) velocities were –3 and +5 km s^{-1}, respectively, each with an uncertainty of $\pm$2 km s^{-1}, on UT 2012 December 21. This velocity difference is less than the ~20 km s^{-1} difference expected, if these lines simply arose from equal mass components, per the Stefanik et al. (2010) orbital solution (see below).

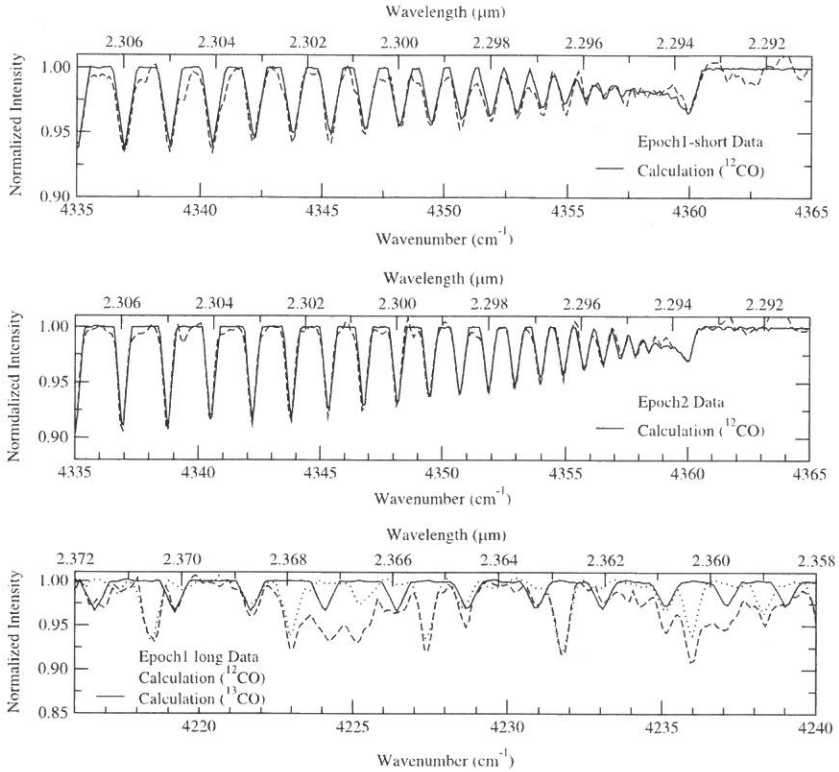

Figure 4. Comparison of observations with LBLRTM line synthesis: top panel, the first epoch ^{12}CO 2-0 bandhead and LBLRTM fitted with $T = 1300$ K and $\log N = 19.9$ cm^{-2} for an assumed 1 AU path across the disk (see text); middle panel, second epoch ^{12}CO 2-0 bandhead fitted with $T = 1100$ K and $\log N = 20.1$ cm^{-2}; bottom panel, first epoch longwave data fitted with ^{13}CO 2-0 lines with $T = 1300$ K, $N = 19.9$ cm^{-2} and ^{12}C/^{13}C = 5. The other, narrow lines are ^{12}CO, plus two broader H-Pfund features at 4225 and 4236 cm^{-1}.

At least eight weak emission lines, at 3.988, 3.998, 4.001, 4.013, 4.029, 4.035, 4.038, and 4.062 μm, are present—see Figure 3. The first of these appears to be double. One weak absorption line is also present, at 3.992 μm. All but those at 4.029, 4.035, and 4.038 μm are clearly absent in the raw spectrum of the telluric standards and thus must arise in ϵ Aur. The above three wavelengths are in a region of prominent absorption by telluric N_2O lines, and thus their precise wavelengths and their realities are less certain.

However, as there are no obvious residuals in the reduced spectrum in line-free regions at many other wavelengths corresponding to comparably strong telluric N_2O lines, we believe that they also are real and arise in ϵ Aur. Based on the NIST atomic line database, we could make no high confidence identification for these lines, except for the blend at 3.986 μm, which is likely due to Na I. Lines of that species also are seen weakly in emission at 2.2062 and 2.2089 μm in the spectra of Stencel et al. (2011). The wavelengths of the other lines have plausible matches with four Si I (7 eV) lines, two Fe I (7 eV) lines and four C I (10 eV) lines.

4. ANALYSIS

4.1. The New CO Spectra

Our first GNIRS spectrum, 2011 January 4 (on RJD 55565, where RJD = JD-2,400,000), was obtained during totality, but 165 days after mid-eclipse and 55 days prior to third contact. It contains numerous lines of CO, beginning at the 2.29345 μm 2–0 bandhead, and filling the spectrum to the long wavelength limit of observation on that date, 2.3725 μm. Isolated lines of the ^{12}CO 2–0 band that were detected include R0 up to about R40, plus P branch lines P0–P10, with line depths of 7% or less. These weak lines with depths of less than 10% appear to be optically thin with limited spectral resolution—although our model shows them to be saturated at their point of origin (see below). Observed lines of ^{12}CO 3–1 include R2–R32, with lines depths of 4% or less. After correcting for the Pfund line profiles, the strongest remaining features include lines of ^{13}CO 2–0 R16–R35, with line depths of 2% or less. Based on the eclipse light curve and interferometric imaging (Kloppenborg et al. 2010), the observation occurred during a phase of maximum photometric eclipse, when the disk still spanned the entirety of the F star's southern hemisphere, leaving the F star's northern hemisphere as the continuum light source—suggesting the appearance of CO absorption arises in atmospheric layers above the optically thick disk.

The CO lines in the first epoch (nearer mid-eclipse) appear shallower and slightly less blueshifted (–35 km s^{-1} after heliocentric correction) than lines seen in the later epochs, which were further blueshifted to –43 and –45 km s^{-1}. The latter observations followed third contact when the disk no longer maximally eclipsed the F star. These second and third epoch spectra—2011 March 30 (RJD 55650, 30 days after third contact), and 2011 April 12 (RJD 55,663, 43 days after third contact)—were obtained during an interesting *still-stand* in the ascending light-curve between RJD 55650–55700—see Figure 5 in Stencel (2012). The ^{12}CO 2–0 lines are deeper (up to 11%) and slightly more blueshifted than during the first epoch. Similar behavior is seen in the ^{12}CO 3–1 lines, reaching up to 5% line depth, and the ^{13}CO 2–0 lines reaching up to 6%

line depth. During third contact, low excitation optical metal spectral lines also show a blueshifted component indicative of a mass-transfer stream at this phase (discovered by Griffin & Stencel 2013 and explored by Sadakane et al. 2013). Transient absorption lines were reported, appearing only between third and fourth contacts, RJD 55618–55710, with a mean velocity of $-39.5 \pm 0.13 > \mathrm{km\,s^{-1}}$, and interpreted as a mass transfer stream distinct from the disk body. This observational phase involves the end of total eclipse and is suggestive of a diffuse cloud trailing the disk. Such a zone would also be fully exposed to F star radiation, unlike the more shielded portions of the disk (as seen from Earth during mid-eclipse), and thus may exhbit a modified local thermal environment. Future models of the system will need to include both the CO appearance and the effects of the mass transfer stream during third contact.

4.2. Comparison with Spectra from the Previous Eclipse

The appearance of transient carbon monoxide was discovered by HS87 during the 1984 eclipse of ϵ Aur. Parallel studies of the spectroscopic behavior of ϵ Aur suggest that optical signatures of the disk have remained largely the same over the past four eclipses, spanning nearly 100 yr—see Griffin & Stencel (2013). HS87 reported a strong asymmetry in the strength of CO before and after *mid*-eclipse, being concentrated in the trailing half of the disk, and essentially absent in the leading half. This is analogous to, but more extreme than, the behavior of the neutral sodium and potassium lines (Leadbeater et al. 2012). Using curve of growth methods, HS87 deduced an excitation temperature of 1000 ± 150 K, a maximum column density of 3×10^{20} CO cm^{-2}, and isotopic ratio ^{12}CO/^{13}CO = 10 $\pm$ 3, the latter indicative of nuclear processing that has increased the ^{13}CO abundance.

HS87's four reported epochs with CO detections occurred on RJD 45592, 45605, 45743 and 45812—which we label here as epochs A, B, C and D—and where RJD = JD-2,400,000. When these epochs are translated to the recent eclipse, using our adopted 9890 days orbital period, they become RJD 55482, 55495, 55633 and 55702 respectively. This means that our first epoch (RJD 55565) falls between their epochs B and C, while our second and third epochs (RJD 55650, 55663) fall between their epochs C and D. Our epoch 4 (RJD 56283) was obtained 483 days after eclipse ended (RJD 55800).

HS87 reported that their epoch C featured the strongest CO lines and largest column density, consistent with the largest line depths reported in our second and third epochs, closest to the time of third contact. They also reported line widths decreased from their early epochs (18 km s^{-1} HWHM) to later epochs (12 km s^{-1}). While GNIRS resolution is less than that of HS87 (16 versus 4.9 km s^{-1}), we partially resolved CO lines to have observed widths of 20 km s^{-1}, implying instrinic line broadening of 12 km s^{-1}, consistent with HS87. If these line widths arise from local turbulence, this may be dynamically significant, being a substantial fraction of the $\sim$35 km s^{-1} rotation rate of the disk. HS87 also reported heliocentric-corrected velocities based on the CO lines at their four epochs as –24.2, –27.2, –44.2 and –43.8 ($\pm$0.4) km s^{-1}, which appear very consistent with our findings, –34 (epoch 1) and –43, –45 km s^{-1} (epochs 2, 3). Taken together, these velocities correspond well with those reported by Leadbeater et al. (2012—their Figure 6) for the disk tracer line K I at 7699 Å, suggestive of disk rotation rates. This also suggests that the presumed irradiated particulate source of the CO responds to the same gravitational potential as does the putative surface spallation that gives rise to the Na I and K I absorption (see Seager & Sasselov 2000; Schaefer & Fegley 2009). The strongest lines reported by HS87 showed an equivalent width of $\sim$0.2 Å, comparable to our numbers. They also reported resolving the CO lines in the earliest phases, but with higher resolution than available to us. Overall, it seems reasonable to conclude that the behavior of transient CO is very similar between these two eclipses, 27 yr apart, and thus providing some constraints on disk replenishment and dissipation timescales.

As the disk moved out of the line of sight and the CO lines disappeared, only F star features remained. We re-observed the system in 2012 April, our epoch 4, thanks to an allocation of Director's Discretionary Time. These new data allowed us to remove the Pfund line contribution and thus confirm the presence of ^{13}CO in the earlier disk phase spectra, at a level consistent with nuclear enhancement. A useful discussion of contribution of Pfund lines to CO overtone line spectra is given by Kraus et al. (2013).

4.3. Spectrum Synthesis

To quantify the conditions under which the CO lines form, we adopted a method long used in atmospheric science and more recently for exoplanet atmospheres (see Brogi et al. 2014), called the Line By Line Radiative Transfer Model, LBLRTM (Clough et al. 2005). This code involves the widely known HITRAN and HITEMP molecular databases (Rothman et al. 2009, 2010). As a first approximation, and to avoid disk scale-size ambiguities related to the uncertain distance to the system, we set the path length at 1 AU, and for that path varied the column density, temperature, and ^{12}C/^{13}C isotopic ratio in a uniform slab model atmosphere, to match the observed line depths (abundance), line ratios (temperature), and bandheads for the ^{12}CO 2–0, ^{12}CO 3–1 and ^{13}CO 2–0 spectra by minimization of residuals—see Figure 4. Note that in Figure 4, persistent hydrogen Pfund lines add to the overall absorption pattern.

Our model uses a temperature and column density to fit the observed profiles, the latter being the product of density times a path length. We chose a representative 1 AU path length because of the uncertainties in the physical dimensions in the ϵ Aur system. Angular sizes in this system are reasonably well determined by interferometry, but the distance to the system remains uncertain by a factor of two (650–1200 pc). The disk radius is estimated to be 4–8 AU, but the CO column path length depends on the chord across the disk—given that our observations occur at phases after mid-eclipse and near third contact, in which case the path length is less than the disk radius. Also, there remain unknowns about disk geometry (is it a symmetric annulus?) and the atmospheric scale height above/below the infrared-opaque disk. Hence, by adopting a 1 AU reference length, and as future work reduces the uncertainty about the distance and physical dimensions involved, our findings can be scaled accordingly.

Results of our spectrum fitting include that the log N_{CO} column density (cm^{-2}) for epoch 1 is 19.90 ± 0.02 at 1275 ± 25 K, and for both epochs 2 and 3, it is slightly higher, 20.13 ± 0.05, but with a cooler 1050 ± 25 K solution. HS87 deduced similar values, using a slab model and curve of growth method, with their log N_{CO} values ranging between 19.4 and 20.5, and a single temperature, $1000\,\mathrm{K} \pm 150\,\mathrm{K}$, spanning all four epochs

that showed CO in their series of spectra. We note that under these conditions, we compute that many of the moderate J lines of ^{12}CO 2–0 would be very narrow and slightly saturated ($\tau \sim 2$), if viewed with unlimited spectral resolution. However, even if saturated, these narrow-lined CO bands collectively absorb relatively little of the continuum radiation and thus have limited effect on the disk thermal equilibrium.

For AU-size lines of sight through the disk, CO molecular density values of 5 to 9 × 10^6 cm^{-3} are implied, and assuming solar C abundance (see Sadakane et al. 2010), yield n_H ~3 × 10^{10} cm^{-3}. Our implied isotopic ratio for best fit to ^{13}CO transitions is ^{12}C/^{13}C = 5 ± 1 for epoch 1, consistent with the HS87 result of 10 ± 3. The models of *single* stars with rotation, by Ekstrom et al. (2012), indicate that stars more massive than 9 solar masses will generate single digit ratios of ^{12}C/^{13}C over evolutionary timescales of less than 35 Myr.

4.4. Brackett α

The persistence of emission in Brackett α in all reported spectra, plus in our new one, argues for the recombination origin of the line from a source substantially hotter than the 7500 K F star. Backman et al. (1985) reported emission in Br α and transient emission in the absorption core of Br γ during eclipse. They interpeted the same as originating in a flow, rather than Keplerian motion associated with either stellar component. Our observation is consistent with their conclusion, except insofar as the disk-centered star would be the more massive component and thus show a small radial velocity offset relative to F star photospheric lines. In our spectra, the absorption wings of Br α are detected, consistent with expectation for the F star, and offset redward of the emission core. Further observations at additional orbital phases will be needed to explore the radial velocity variation of the Br α emission and to establish connection with either a disk-centered star or with a flow/shock nearer the inner Lagrangian point.

5. CONCLUSION

We have shown that infrared spectral lines of CO appeared during the latter phases of the 2009–2011 eclipse of ε Aur due to a transiting disk, and that the line strengths and velocities closely resemble the discovery observations during the latter part of the previous 1982–84 eclipse, indicating disk structure stability on an orbital timescale. We confirm with spectrum line synthesis the result of Hinkle & Simon (1987) that the ^{12}C to ^{13}C ratio is ~5–10, much less than solar (89), thus indicating nuclear processing of material in the system has occured, consistent with dredge-up related to core helium burning. We have also observed the persistent Brα emission post-eclipse to determine whether it traces the motion of the companion star, but found the emission source appears to arise nearer the center of mass than expected from orbital solutions. Continuing observations are essential to confirm and extend this latter result.

Looking forward to the next eclipse cycle (2036-2038), we urge observers to be prepared to observe the transient CO lines with greater phase coverage, in order to map disk structure and especially to monitor third contact and the stream passage phases—seen most recently around JD 2,455,620 ± 10 and 2,455,675 ± 25, respectively. Those dates translate to the next eclipse as JD 2,465,510 (2038 March 27) and 2,465,565 (2038 May 21)—the latter being unfortunately close to solar conjunction.

R.E.S. is grateful to the bequest of William Herschel Womble for support of Astronomy at the University of Denver, along with NSF grant AST 10-16678 to the University of Denver, which provided partial support for this work. He thanks Kathleen Geise and Brian Kloppenborg for useful discussions and the referee for insightful comments, and appreciates the hospitality extended by Gemini-Hilo staff during a 2012 research visit. This work is based on observations obtained at the Gemini Observatory, which is operated by the Association of Universities for Research in Astronomy, Inc., under a cooperative agreement with the NSF on behalf of the Gemini partnership: the National Science Foundation (United States), the National Research Council (Canada), CONICYT (Chile), the Australian Research Council (Australia), Ministério da Ciência, Tecnologia e Inovação (Brazil) and Ministerio de Ciencia, Tecnología e Innovación Productiva (Argentina). We are grateful to the staff of Gemini for its support, and to the people of Hawai'i for enabling observations to be conducted from atop Mauna Kea.

REFERENCES

Backman, D., Simon, T., & Hinkle, K. 1985, PASP, 97, 1163
Brogi, M., de Kok, R., Birkby, J., Schwarz, H., & Snellen, I. 2014, A&A, 565, 124
Clough, S. A., Shephard, M. W., Mlawer, P., et al. 2005, JQSRT, 91, 233
Ekstrom, S., Georgy, C., Eggenberger, P., et al. 2012, A&A, 537, 146
Griffin, R. E. M., & Stencel, R. 2013, PASP, 125, 775
Hajduk, M., Zijlstra, A., & Gesicki, K. 2008, A&A, 490, L7
Herbst, W., Hamilton, C., Leduc, K., et al. 2008, Natur, 452, 194
Hinkle, K., & Simon, T. 1987, ApJ, 315, 296
Hoard, D., Lajdal, D., Stencel, R., & Howell, S. 2012, ApJ, 714, 549
Kloppenborg, B., Stencel, R., Monnier, J., et al. 2010, Natur, 464, 870
Kraus, M., Oksala, M., Nickeler, D., et al. 2013, A&A, 549, A28
Leadbeater, R., Buil, C., Garrell, T., et al. 2012, JAAVSO, 40, 729
Mantz, A. W., Maiilard, J. P., Roh, W. B., & Rao, K. N. 1975, JMoSp, 57, 155
Rothman, L., Gordon, I., Barbe, A., et al. 2009, JQSRT, 110, 533
Rothman, L., Gordon, I., Barber, R., et al. 2010, JQSRT, 111, 2139
Sadakane, K., Kambe, E., Sato, B., et al. 2010, PASJ, 62, 1381
Sadakane, K., Kambe, E., Hashimoto, O., et al. 2013, PASJ, 65, L1
Schaefer, L., & Fegley, B. 2009, ApJL, 703, L113
Seager, S., & Sasselov, D. 2000, ApJ, 537, 916
Stefanik, R., Lovegrove, J., Pera, V., et al. 2010, AJ, 139, 1254
Stencel, R. 2007, IAU Symp., 240, 202
Stencel, R., Kloppenborg, B., Wall, R., et al. 2011, AJ, 142, 174
Stencel, R. 2012, JAAVSO, 40, 618
Takeuchi, M. 2011, PASJ, 63, 325
Williams, J., & Cieza, L. 2011, ARA&A, 49, 67